4

Approach safety and collision avoidance

The objective of this chapter is to explain the requirements for trajectory safety, to discuss the causes for trajectory deviations due to the orbital environment and to imperfections and errors of the onboard system, and to investigate the possibilities of employing protection against trajectory deviations. The discussions concerning trajectory deviations and trajectory safety concentrate on the rendezvous phases, since the mission phases of launch and phasing are generally controlled by operators or computer functions on ground. In the rendezvous phases the two spacecraft are relatively close together, their orbital planes are well aligned and the trajectory of the chaser, by definition, leads toward the target, so that any deviation from the planned trajectory can potentially lead to a collision, directly or after one or more orbital revolutions.

4.1 Trajectory safety – trajectory deviations

Rendezvous and docking is in fact a 'planned collision' of two spacecraft, which is controlled by considering the geometric location of the contact points on the two vehicles and the linear velocities and angular rates at contact. To achieve the contact conditions within the allowed margins, the trajectories have to be maintained within close tolerances prior to contact. Any deviation from such tolerances may lead either to a loss of the rendezvous and mating opportunity or even to the danger of collision of the two spacecraft at unsuitable points and dynamic conditions, with the risk of serious damage. For this reason, rendezvous operations, and all functions and systems involved in them, have to comply with failure tolerance and safety requirements.

The level of failure tolerance required for safety and mission success depends on the type of mission. The term *safety* is used in the context of space operations usually for the

safety of human life. It is, therefore, only applicable to missions involving at least one manned vehicle, which could be either the target or chaser vehicle. These missions require the highest level of failure tolerance. Failure tolerance requirements of unmanned missions are lower or, at most, equal to those of manned missions. Instead of *safety of human life*, the most important protection in unmanned missions must be given to the investment made in the missions of the two spacecraft involved. For this issue, instead of *safety* the term *spacecraft security* has been proposed by some authors. However, as there is no difference between manned and unmanned missions when considering the effects of trajectory deviations and the danger of collision, it would lead only to confusion if different terms were to be used in the two cases for the same problem. The terms *approach/departure safety* and *trajectory safety* will, therefore, be used in the following regardless of whether a manned or an unmanned mission is under discussion.

4.1.1 Failure tolerance and trajectory design requirements

Failure tolerance requirements are usually defined for general application, i.e. for all systems of the vehicle(s) and for all payloads in a given mission scenario. They need to be interpreted, however, on considering their consequences for each particular application. For example, in the International Space Station (ISS) Programme the following requirements have been defined (NASA 1998b).

(1) No single failure shall cause major consequences.

(2) No combination of two failures shall have catastrophic consequences.

A *single failure* is defined as 'the inability of either a system, subsystem or item (hardware and software) to perform its required function', or as any 'operator failure'; a *major consequence* is defined as 'the loss of the particular mission', e.g. of the rendezvous mission of another vehicle with the ISS; and a *catastrophic failure* is defined as either 'loss of life or disabling injury of crew', or 'loss of the space station or of one of its major elements'.

For spacecraft operations this can be translated into the familiar *fail operational–fail-safe* requirement. It can be expected that such a two-level requirement would also be applicable for, e.g., the case of a satellite servicing mission by an unmanned servicing vehicle, which is a typical rendezvous and capture mission scenario with two unmanned vehicles. For the rendezvous and capture operations proper, these failure tolerance requirements can be interpreted in the following way.

- *Approach up to contact*

  After one failure the trajectory must remain safe (collision-free), and it must be possible to continue or resume the rendezvous mission.

  After two failures the resulting trajectory must be collision-free, without requirement to continue the mission.

- *Capture*

  After one failure the approaching vehicle must be able to retreat and re-try.

  After two failures the chaser vehicle must be able to leave the target safely (collision-free), without requirement to resume the mission.

- *Departure*

  After one failure the chaser vehicle must be able to continue the nominal departure and de-orbitation operations.

  After two failures the chaser vehicle must be able to leave the target safely (collision-free), without further requirements.

A more detailed interpretation of failure tolerance requirements for other rendezvous related mission phases, such as structural connection/disconnection and operations preparing the attached phase, is not needed for the purpose of this book, as they are in no way different from other operations aboard a spacecraft.

4.1.2 Design rules for trajectory safety

For the approach phase it will be indicated in the following how such safety requirements can be translated into design requirements for the approach trajectory strategy and for the onboard system.

(1) The approach and departure strategies and their trajectory elements must be designed to be as safe as possible concerning the risk of collision. This means that, the natural development of each trajectory element shall be collision-free for as long as possible, taking into account all possible dispersions and including the possibility of a failure of the onboard system. This is of course not possible up to the end, as eventually the chaser vehicle will make physical contact with the target vehicle.

(2) In the vicinity of the target station, the onboard system of the chaser must be able to monitor the relative state vector w.r.t. the target at each point along the trajectory, and must be able to correct it automatically when deviations from the planned trajectory become too large.

(3) The onboard system must be able to detect failures of its subsystems, functions or equipment and must be able to engage redundant equipment, functions or subsystems within a time limit, which allows either the continuation of the present trajectory or the initiation of a back-up operation which permits a later resumption of the mission.

(4) In any case, at each point of the approach and departure trajectories, when all control fails and the actual state vector exceeds safety boundaries, the onboard

system must be able to execute an operation which ensures collision avoidance between chaser and target. Where natural collision-free trajectories are available (see (1)), such an operation could simply be the inhibition of all thruster action. In other cases the execution of a single boost may be sufficient to remove the chaser from the target vicinity (see section 4.5).

To be able to assess possibilities and constraints in the trajectory strategy design concerning the implementation of the first of the above design requirements, it will be necessary first to identify the causes of trajectory deviations and thereafter to find suitable safeguards against such deviations. The second and third design requirements regard the design of the automatic onboard control system, which will be discussed in detail in chapter 6. The last of these design requirements, the availability of a safe collision avoidance manoeuvre (CAM), has two implementation aspects:

- the design of the trajectories and manoeuvres for each case, which will be treated in section 4.5;
- the detection of deviations from the planned state vector at any point of the trajectory and the initiation of the appropriate actions, which is the task of the onboard control system, and will be treated in chapter 6.

4.1.3 Causes of deviations from the planned trajectory

Potential causes of deviations of the actual trajectory from the planned one are the following:

- orbital disturbances,
- navigation errors,
- control errors,
- thrust vector errors,
- thruster failures.

Orbital disturbances are forces acting on the spacecraft that change its trajectory, e.g. due to the deviations of the Earth's gravitational potential from a sphere (this plays a role during phasing and very far range rendezvous operations), due to atmospheric drag and solar pressure (this plays a role in all ranges, but not in all altitudes), thruster plume pressure (this plays a role only at very short distances), etc. These disturbances are the subject of the next section.

Navigation errors are the differences between the state as perceived by the onboard system and the real state (position, velocities, attitude, angular rates) of the vehicle. Initial navigation errors can be amplified over time by effects of orbital dynamics and by thrust manoeuvres (see section 4.3.1).

Control errors are the differences between the proper corrections of the values to be controlled and the ones actually produced by the controller. The effects of control errors are due in equal part to navigation errors and to thrust vector errors; therefore they should not be discussed separately.

Thrust vector errors are deviations in magnitude and direction from the assumed applied force and torque vectors (see section 4.3.2) .

Thruster failures could, strictly speaking, also be covered by the term 'thrust vector errors'. However, under this title only hard failures will be discussed, such as thruster valves stuck open and closed, the results of which are much more dramatic and require quite different measures from the small deviations to be treated under 'thrust vector errors'. It is, therefore, kept as a separate category of causes for trajectory deviations (see section 4.3.3).

The most important causes for trajectory deviations will be discussed in more detail in the following sections of this chapter.

4.2 Trajectory disturbances

The intention of this section is to provide an overview of only the most important trajectory disturbances, those which have a significant effect on the rendezvous trajectories, i.e. disturbances after which the spacecraft position is noticeably changed after one or a few orbits. The most significant disturbances depend on the class of orbit in which the rendezvous takes place. In LEO for instance, the most significant disturbance is the drag due to the residual atmosphere and, in the far range of the approach (in particular during phasing), the effect of the geopotential anomaly. In GEO, on the other hand, the most significant disturbance is the pressure of the solar radiation.[1] In both cases, the largest disturbance forces will occur, however, as a result of the pressure of thruster plumes of one vehicle on the surfaces of the other one when the two spacecraft are in close proximity. The disturbance due to the deviation of the gravitational potential of the Earth from a sphere results mainly in a drift of nodes (change of RAAN), which is of importance for the absolute trajectories, e.g. during phasing, but plays a minor role for the relative trajectories between chaser and target during close range operations. The effects of other disturbances on rendezvous trajectories, such as the luni–solar potential and the higher order harmonics of the Earth potential, are orders of magnitude lower.

Expected or known trajectory disturbances can be taken into account and compensated for. The largest uncertainties will occur in the knowledge of the actual values of absolute and differential drag and, for the last tens of metres of the approach, of the plume dynamic forces. Because of the large variation in density of the residual atmosphere over one orbit and over time in general, and because of the variation of the cross section of the spacecraft due to rotating solar arrays, significant uncertainties will always remain for the disturbance by air drag. Large uncertainties will also remain for the

[1] This book concentrates on rendezvous in LEO, where the majority of rendezvous missions are performed.

disturbance by plume forces due to the limited knowledge of the actual pressure distribution in the thruster plumes and due to the modelling errors of the spacecraft surfaces and of their interaction with the pressure fields.

4.2.1 Drag due to residual atmosphere

The drag force by the residual atmosphere acting on a spacecraft is

$$F_{\mathrm{D}} = -\frac{\rho}{2} V_x^2 C_{\mathrm{D}} A \tag{4.1}$$

where $V_x = \omega r$ is the orbital velocity; C_{D} is the drag coefficient; and A is the cross section of the body. As both vehicles are affected by drag, and as the difference of their absolute velocities is negligible, the differential drag force per unit of mass $\gamma_{\mathrm{D}} = \frac{F_{\mathrm{d}}}{m}$ acting on the chaser w.r.t. the target in a circular orbit is

$$\Delta\gamma_{\mathrm{D}} = \gamma_{\mathrm{Dc}} - \gamma_{\mathrm{Dt}} = -\frac{\rho}{2}\omega^2 r^2 \left(\frac{C_{\mathrm{Dc}} A_{\mathrm{c}}}{m_{\mathrm{c}}} - \frac{C_{\mathrm{Dt}} A_{\mathrm{t}}}{m_{\mathrm{t}}} \right) \tag{4.2}$$

where m is the mass of the vehicles and the indices c and t indicate chaser and target, respectively. The relation

$$C_{\mathrm{B}} = \frac{m}{C_{\mathrm{D}} A}$$

is called the ballistic coefficient of the vehicle. With this term, which is often used in rendezvous analysis, the equation becomes

$$\Delta\gamma_{\mathrm{D}} = -\frac{\rho}{2}\omega^2 r^2 \frac{1}{C_{\mathrm{Bc}}} \left(1 - \frac{C_{\mathrm{Bc}}}{C_{\mathrm{Bt}}} \right) \tag{4.3}$$

The effect of this disturbance on the trajectory can be calculated by introducing the value for $\Delta\gamma_{\mathrm{D}}$ as γ_x into Eqs. (3.59) and (3.66). For a more detailed model, not only the cross section of the vehicle, but the individual surfaces and their direction w.r.t. the orbital velocity vector, have to be taken into account.

The atmospheric density ρ is the value known with least accuracy in this equation. If the value for a certain orbital height is known, it can be modelled locally around this point by an exponential function:

$$\rho(z) = \rho(z_0) \mathrm{e}^{\frac{z - z_0}{H(z_0)}} \tag{4.4}$$

where $H(z_0)$ is a scale height coefficient (Carrou 1995). The atmospheric density at a particular height is dependent on the temperature of the atmosphere. For instance, on the side illuminated by the Sun, the atmosphere will expand and denser parts of the atmosphere will rise to higher altitudes. The density at a certain orbital height will, therefore, not be constant but will increase (solar bulge) on the illuminated side of the orbit, and

vice versa on the opposite side. The effect of the solar bulge on the relative motion between the chaser and target vehicles will, however, be much lower than the change of the absolute value of the density, as both vehicles are equally affected. Also, as this effect is periodic with the orbit, for manoeuvres with a transfer time of one revolution, the effect will be averaged out to a large extent. For preliminary trajectory assessments, an orbital average can therefore be assumed. For detailed analysis and simulations, however, the effect of the solar bulge needs to be taken into account.

A large influence on the density of the atmosphere at a certain orbital height is the solar flux, which heats up the outer atmosphere. Three periodic variations of the solar flux effects on the atmosphere can be distinguished:

- a period of about 27 days, which is due to the rotation of the Sun about its axis;
- a period of 1 year, which is due to the change of attitude of the Earth w.r.t. the Sun's axis during one orbit of the Earth around the Sun;
- a period of about 11 years, which is due to the solar activity cycle.

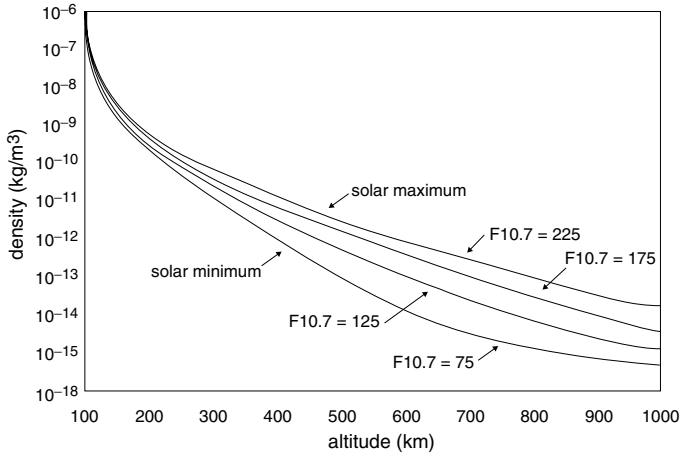

Figure 4.1. Density vs. altitude at various levels of solar flux. Taken from Larson & Wertz (1992), with the kind permission of Kluwer Academic Publishers.

The last effect has the most significant influence. For example, in a 400 km altitude orbit the density can vary between approximately $5 \times 10^{-10}\ \mathrm{kg/m^3}$ at high solar activity and $1 \times 10^{-12}\ \mathrm{kg/m^3}$ at low solar activity. A lot of research work has been performed to provide a model of the atmosphere. Well known are two empirical models: JACCHIA (Jacchia 1977) and MSIS (mass spectrometer incoherent scatter) (Hedin 1986). The variation of the density with the solar flux is shown in figure 4.1, which is taken from Larson & Wertz (1992).

In applications where a complex space station with large surfaces of solar generators and radiators is the target, and relatively compact vehicles comprise the chaser, the ratio of the ballistic coefficients $\frac{C_{\mathrm{Bc}}}{C_{\mathrm{Bt}}}$ can become quite large (4–8). Because of the fact that the solar arrays are pointing toward the Sun, the ballistic coefficient of spacecraft with articulated solar panels will change over one orbit. In cases where solar arrays can be articulated in two axes (to align the pointing axis also with the lateral Sun direction), the ballistic coefficient also varies over the year. If both target and chaser have articulated solar panels, the variation of the ratio of ballistic coefficient will, however, be lower than the variation of the absolute values. Whereas in first trajectory assessments this effect can be neglected, in simulations for performance verification (see sections 10.3.2 and 10.3.3) the variation of the ballistic coefficients must be properly taken into account. To simplify the discussion of the qualitative effects, drag forces are assumed to be constant in the following examples. To demonstrate the effect of the residual atmospheric drag, examples for free drift motions and for motion after impulsive manoeuvres are discussed below.

Free drift motion and impulsive manoeuvres with drag

The first type of trajectory discussed here is the release of a spacecraft on a circular orbit, e.g. from a controlled station keeping to a free motion. Prior to release, the drag force acting on it is counteracted by the control forces. The free drift motion of the spacecraft after release is given by the equations for a constant force transfer, into which the acceleration due to drag has to be inserted. For a trajectory starting in $\boldsymbol{O}_{\mathrm{lo}}$, the equation of motion is thus obtained by inserting Eq. (4.3) into Eqs. (3.59):

$$\begin{aligned} x(t) &= -\frac{\rho}{2}\omega^2 r^2 \frac{1}{C_{\mathrm{Bc}}}\left(1-\frac{C_{\mathrm{Bc}}}{C_{\mathrm{Bt}}}\right)\left(\frac{4}{\omega^2}(1-\cos(\omega t))-\frac{3}{2}t^2\right) \\ z(t) &= -\frac{2}{\omega^2}\frac{\rho}{2}\omega^2 r^2 \frac{1}{C_{\mathrm{Bc}}}\left(1-\frac{C_{\mathrm{Bc}}}{C_{\mathrm{Bt}}}\right)(\sin(\omega t)-\omega t) \end{aligned} \tag{4.5}$$

Since the relative motion between chaser and target is negligible compared with the absolute orbital velocity, the difference of velocity does not enter into the calculation of the drag forces. The results of Eqs. (4.5) can, therefore, be added to the results of the other trajectory cases; e.g., for a trajectory starting on a different altitude from the target orbit, Eqs. (3.25) have to be added to Eqs. (3.59).

The absolute motion of a spacecraft w.r.t. a local orbital frame of constant altitude is obtained by setting the ratio of ballistic coefficients $C_{\mathrm{Bc}}/C_{\mathrm{Bt}} = 0$, i.e. $C_{\mathrm{Bt}} = \infty$. The resulting trajectory is shown in figure 4.2 for a 400 km circular orbit, an assumed drag acceleration of $\gamma_{\mathrm{D}} = -1.38 \times 10^{-6}\ \mathrm{m/s^2}$, which corresponds to a density of about $10^{-11}\ \mathrm{kg/m^3}$ and a ballistic coefficient of $C_{\mathrm{Bc}} \approx 215$, which is valid for a relatively compact spacecraft.

Figure 4.2 shows the beginning of the natural decay (three revolutions) of a satellite orbit due to the drag of the residual atmosphere (note: the Earth is in the +R-bar di-

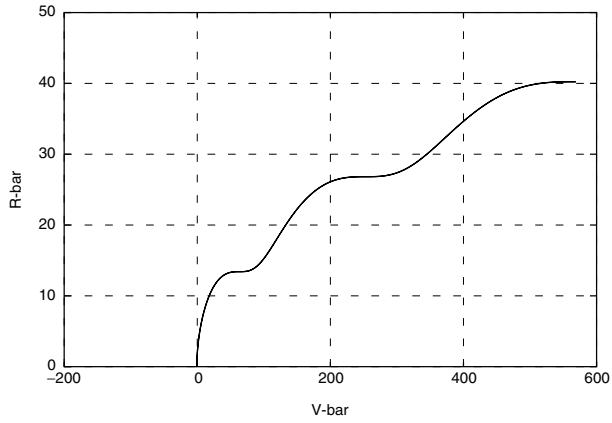

Figure 4.2. Free motion with drag $-1.38 \times 10^{-6}\ \mathrm{m/s^2}$ starting at $\boldsymbol{O}_{\mathbf{lo}}$ (400 km orbit, three revolutions).

rection). The sinusoidal component of the trajectories in figures 4.2 and 4.3 is due to the fact that the drag force is added at the starting point as a step function (release from station keeping).

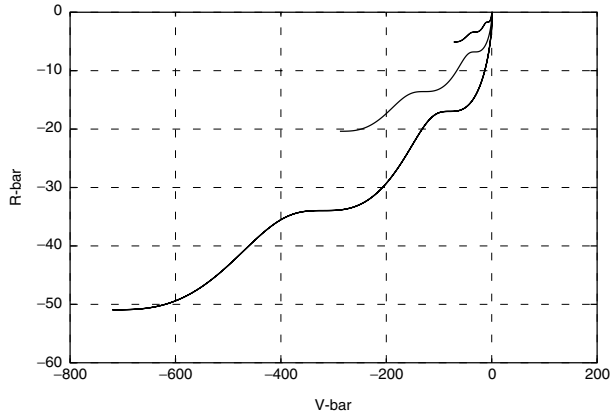

Figure 4.3. Example: motion with differential drag (start: $\mathbf{O}_{\mathrm{lo}}$, $C_{\mathrm{Bc}}/C_{\mathrm{Bt}} = 1.5, 3, 6$).

If chaser and target have the same ballistic coefficient, no effect will be seen in the target-centred orbital frame. However, if, e.g., the target has a lower ballistic coefficient, i.e. a higher resistance, it will decay faster than the chaser, causing the chaser to move over time to a higher position (−R-bar direction) behind the target. This is the case for the examples shown in figure 4.3, which are calculated for three orbital revolutions and for the same altitude and density as in figure 4.2. The ballistic coefficient of the chaser

of $C_{\mathrm{Bc}} = 470\ \mathrm{kg/m^2}$ is that of a very compact vehicle. The ratio of the ballistic coefficients $C_{\mathrm{Bc}}/C_{\mathrm{Bt}}$ has been varied between 1 and 6, with the higher values belonging to a target with larger (or chaser with smaller) surfaces. The results demonstrate the importance of the differential drag effect on the development of the free drift motion between chaser and target. Starting on the target orbit, a free drifting chaser with a ballistic coefficient only 1.5 times as large as that of the target vehicle would have reached, after three orbital revolutions, a position of about 5 m above and 70 m behind the target.

As a second case, the effect of differential drag on trajectories after impulsive manoeuvres will be analysed. The equations of motion for a tangential impulse manoeuvre with drag can be obtained by adding to Eqs. (3.28), for the impulsive manoeuvre, the above derived Eqs. (4.5), for free motion with constant drag force. Correspondingly, the equations for a radial impulse manoeuvre with drag are obtained by adding Eqs. (4.5) to Eqs. (3.34) for the impulsive radial manoeuvre.

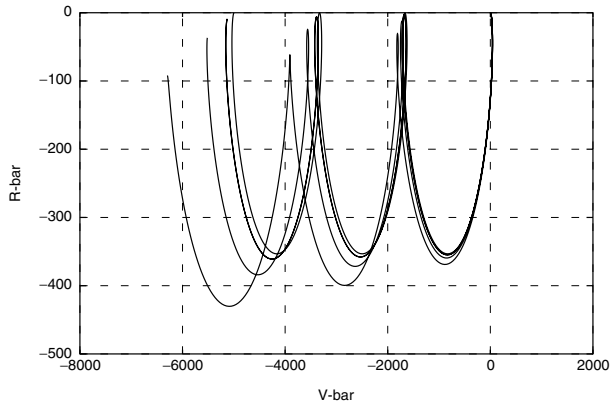

Figure 4.4. Tangential impulse 0.1 m/s with differential drag (400 km, $C_{\mathrm{Bc}}/C_{\mathrm{Bt}} = 1, 1.5, 3, 6$).

Results are shown for a manoeuvre with a tangential initial impulse in figure 4.4 and for a manoeuvre with a radial initial impulse in figure 4.5, assuming the same conditions as for figure 4.3 above. The absolute change of position is the same for all cases with the same density and ballistic coefficient and is equal to that of the drift case (figure 4.3). The relative effect is, however, larger on the radial impulse manoeuvre than on the tangential one, as a radial impulse of the same magnitude produces roughly a five times lower maximum change of position than a tangential manoeuvre.

4.2.2 Disturbances due to geopotential anomaly

Due to the fact that the shape of the Earth deviates from an ideal sphere, and that its mass is not distributed homogeneously inside its body, the gravitational forces are not entirely directed toward the orbit centre, but can have components in other directions in

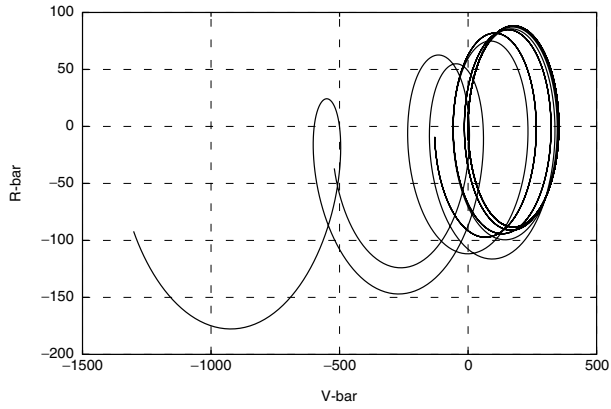

Figure 4.5. Radial impulse 0.1 m/s with differential drag (400 km, $C_{\mathrm{Bc}}/C_{\mathrm{Bt}} = 1, 1.5, 3, 6$).

and out of the orbit plane. These forces will vary over one orbital revolution and can cause changes in the orbital parameters. The gravitational potential of the Earth can be approximated by the function

$$\Phi = \frac{\mu}{r}\left(1 - \sum_{n=2}^{\infty} J_n \left(\frac{R_{\mathrm{E}}}{r}\right)^n P_n(\sin\varphi)\right) \tag{4.6}$$

where J_n are harmonic coefficients of the potential, R_{E} is the Earth radius at the equator, r is the distance of the satellite from the centre of the Earth, P_n are Legendre polynomials, φ is the latitude and μ is the gravitational constant of the Earth. This approximation uses only the zonal deviations from the sphere, i.e. the ones depending on the latitude. More elaborate models include also the sectoral (depending on longitude) and tesseral (combined zonal and sectoral) terms, which are, for most cases of trajectory analysis and particularly for the relatively short duration of a rendezvous mission, of low importance. A detailed discussion of the modelling of the gravitational potential of the Earth can be found in many textbooks, e.g. Carrou (1995).

The most significant effect on near Earth orbits is caused by the second harmonic of the Earth potential, which represents the Earth's oblateness. The coefficient J_2 is more than two orders of magnitude larger than all other ones, hence the name J_2-effect for the most significant gravitational disturbance. Seen in the $\boldsymbol{F}_{\mathbf{eq}}$ frame, the effect of the oblateness of the Earth on the orbits results in the following motions:

- a motion of the line of nodes, i.e. a change over time of the RAAN ($\dot{\Omega}$), called the 'drift of nodes' or 'regression of nodes',
- a rotation of the line of apsides ($\dot{\omega}$) for an elliptical orbit.

Although most rendezvous missions take place in near circular orbits, both effects are of importance for rendezvous operations during phasing and far range rendezvous manoeuvres, where elliptical orbits are often used. For circular orbits the absolute value of the regression of nodes remains significant and has to be taken into account for all issues depending on absolute orbit development, such as ground track, communication windows with relay satellites, GPS satellite visibility and illumination conditions. The difference between the regression of nodes of chaser and target orbit, however, will decrease and eventually disappear when the two vehicles come close to each other.

In the literature (e.g. Wertz & Larson 1994) the following formulas are given for the rate of change of the line of nodes and the line of apsides:

- regression of nodes:

$$\begin{aligned} \dot{\Omega}_{J2} &= -1.5nJ_2(R_\mathrm{E}/a)^2(\cos\, i)(1-e^2)^{-2} \\ \dot{\Omega}_{J2} &\approx -2.06474 \times 10^{14} a^{-7/2}(\cos\, i)(1-e^2)^{-2} \end{aligned} \tag{4.7}$$

- rotation of line of apsides:

$$\begin{aligned} \dot{\omega}_{J2} &= 0.75nJ_2(R_\mathrm{E}/a)^2(4-5\,\sin^2 i)(1-e^2)^{-2} \\ \dot{\omega}_{J2} &\approx 1.03237 \times 10^{14} a^{-7/2}(4-5\,\sin^2 i)(1-e^2)^{-2} \end{aligned} \tag{4.8}$$

where n is the mean orbital motion in deg/day, R_E is the Earth radius at the equator, a is the semi-major axis in kilometres, e is the eccentricity and i is the inclination. The results $\dot{\Omega}$ and $\dot{\omega}$ are in degrees per day. As already mentioned, the rotation of the line of apsides is, for a rendezvous mission, of lower importance, as long as the target is on a quasi-circular orbit.

Examples

For a circular orbit of, e.g., 400 km altitude and 52 deg inclination (International Space Station), the regression of nodes would be, according to Eq. (4.7) $\dot{\Omega}_{J_2} = -4.989$ deg/day. For an elliptic phasing orbit of, e.g., 350/200 km apogee/perigee height, the regression of nodes would be $\dot{\Omega}_{J_2} = -5.326$ deg/day.

For an inclination of 28.5 deg (Cape Canaveral launches), but otherwise the same orbit relations, the drift of nodes would be $\dot{\Omega}_{J_2} = -7.121$ deg/day for the 400 km altitude circular orbit and $\dot{\Omega}_{J_2} = -7.603$ deg/day for the 350/200 km elliptic phasing orbit.

4.2.3 Solar pressure

Solar radiation produces a force on a spacecraft in the Sun–satellite direction:

$$\vec{F}_\mathrm{SP} = -p \cdot A \cdot \vec{u}_\mathrm{S} \tag{4.9}$$

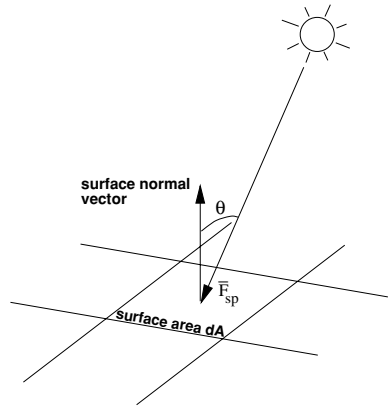

Figure 4.6. Solar pressure force on surface area.

Per unit of mass of the satellite this is

$$\vec{\gamma}_{\mathrm{SP}} = -p\frac{A}{m}\vec{u}_{\mathrm{S}} \tag{4.10}$$

where p is the radiation momentum flux, A is the cross section of the satellite, m is the mass of the satellite and $\vec{u}_{\mathrm{S}}$ is the Sun–satellite direction unity vector. The radiation momentum flux varies periodically with the orbit of the Earth around the Sun and is

$$p = 4.38 \times 10^{-6}\ \mathrm{N/m^2} \text{ at aphelion}$$
$$p = 4.68 \times 10^{-6}\ \mathrm{N/m^2} \text{ at perihelion}$$

As the forces due to solar pressure have in- and out-of-plane components, depending on the Sun direction w.r.t the orbital plane, the solar pressure will have some effect on all orbital parameters, with the most important ones being on eccentricity and on inclination. Depending on orbital height and Sun direction, the force will be intermittent, i.e. the force will be zero when the satellite is in the shadow of the Earth.

Solar pressure is the most prominent disturbance for rendezvous trajectories in geosynchronous orbits, where drag is practically zero but where solar pressure, in combination with a difference in the ballistic coefficients of chaser and target vehicles, can lead to different accelerations of the two. Because the Sun–satellite direction varies along the orbit and with the year, the actual effects of solar pressure need to be calculated separately for each case. In a more detailed analysis, and for verification purposes, the individual surfaces of the satellite body have to be taken into account concerning their direction w.r.t. the Sun–satellite vector and their reflection properties, i.e. whether absorptive, diffuse reflective or specular reflective.

In a 400 km altitude orbit, the acceleration due to solar pressure and the resulting

effect on the rendezvous trajectories is about two to three orders of magnitude lower than that of atmospheric drag.

4.2.4 Dynamic interaction of thruster plumes between chaser and target

Plume interaction becomes an important disturbance when spacecraft are operating in close proximity. Depending on the size of the thrusters and the geometric extension of the opposite spacecraft's surfaces, the effects are significant in a range below a few tens of metres through a few hundred metres. As thruster plumes are limited in their extension, and since the various spacecraft surfaces are at those distances equal to or larger than the plume diameter, there is no possibility of treating the disturbance more globally, as can be done for air drag or solar pressure. Rather, the forces must be integrated over the various surfaces, taking into account the thrust direction w.r.t. the particular surface and the pressure distribution of the plume as a function of range and angle from the centre line.

The force exerted by a thruster plume on a surface element $\mathrm{d}S$ can be described by the plume pressure $P(r, \theta)$ and the direction γ of the gas flux w.r.t the surface:

$$\mathrm{d}F = -P(r, \theta) \cos\gamma \, \mathrm{d}S \tag{4.11}$$

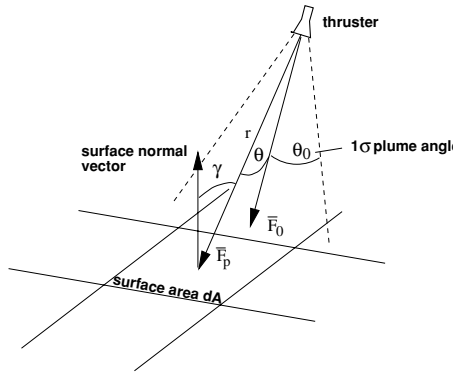

Figure 4.7. Thruster plume force on surface area.

A model of the pressure in a thruster plume as a function of the range r and the angle from the centre line θ has been given in Desplats (1988) by the following equation:

$$P(r, \theta) = \frac{\phi_0}{r^2} \, \mathrm{e}^{\frac{-\theta^2}{2\theta_0^2}} \tag{4.12}$$

where ϕ_0 is a flux constant characterising the thruster, θ_0 is the half cone angle, representing the 1σ value of the gas jet (assuming a Gaussian distribution), i.e. 3σ or 99.7 %

of the plume cross section is covered at $3\theta_0$. The value of ϕ_0 as a function of the standard deviation cone angle θ_0 can be computed from the following force conservation law:

- The force exerted by the plume on a unit sphere of 1 m range around the thruster must be equal to the thrust level F_0 of the thruster.

Integrating Eq. (4.11) over the surface of the unit sphere with the pressure profile of Eq. (4.12) yields, for the characteristic flux,

$$\phi_0 = \frac{F_0}{\pi} \frac{1}{\int_0^{\pi} (\mathrm{e}^{-\frac{\theta^2}{2\theta_0^2}} \sin(2\theta) \mathrm{d}\theta)} \tag{4.13}$$

The model has been validated for the Hermes–Columbus Free-Flyer scenario in Retali (1990) Typical values of the 1σ half cone angle θ_0 are of the order of 13 deg.

Accelerations due to plume interaction from one spacecraft on another one can (at short distance) be one to two orders of magnitude higher than that of air drag. Braking boosts close to the spacecraft, where the plume is directed toward the target vehicle, must therefore be avoided. Attitude control thrust could be in all directions, but the single thrusts are relatively short in time. Force and torques exerted on the target vehicle by such thrusts can properly be evaluated only by closed loop simulation of the chaser GNC operation, with detailed modelling of spacecraft geometry, thruster locations and thruster plumes.

4.3 Trajectory deviations generated by the spacecraft systems

The following discussion of trajectory deviations, caused by errors of systems or equipment, assumes that all manoeuvres are performed in open loop. The intention is, for each type of error to establish equations, which allow the assessment of type and magnitude of the trajectory deviation caused. Numerical examples are given to provide an understanding of the magnitude of the error effects.

4.3.1 Trajectory deviations due to navigation errors

As stated in section 4.1.3, navigation errors are the deviations of the measured or predicted state vector of the vehicle from the real one. Such deviations can result from alignment errors between the sensor and the spacecraft axes, from measurement performance limitations of the sensors used (see chapter 7), from aberrations caused by the measurement environment, and from performance limitations of the information processing in the navigation filter (see section 6.2.1). The parameters to be measured are position, linear velocities, attitude and angular rates. The following discussion will identify the trajectory uncertainties and errors, which may occur as a result of such measurement errors after a certain time of motion.

Position measurement errors

Position measurement errors in the x-direction have no further effects on the trajectory development than the position error itself. Position errors in the y-direction will result, according to Eqs. (3.27), in a sinusoidal development of the error over time. Position errors in the z-direction can have two effects depending on the x-velocity at measurement: either they will result, according to Eqs. (3.25), in an error of the velocity in the x-direction without further errors in z, or they will result, according to Eqs. (3.26), in a looping motion with significant z excursions.

- Measurement error $\Delta x_{\mathrm{m}} \Longrightarrow$ trajectory error of

$$\Delta x_{\mathrm{m}} \tag{4.14}$$

- Measurement error $\Delta y_{\mathrm{m}} \Longrightarrow$ trajectory error of

$$\Delta y(t) = \Delta y_{\mathrm{m}} \cos(\omega t) \tag{4.15}$$

- Measurement error $\Delta z_{\mathrm{m}} \Longrightarrow$ trajectory error of

$$\Delta x(t) = \frac{3}{2}\omega \Delta z_m t \tag{4.16}$$

  if the chaser is on a circular orbit below or above the target orbit, i.e. moving with the velocity belonging to this orbit.

- Measurement error $\Delta z_m \Longrightarrow$ trajectory errors of

$$\begin{aligned} \Delta x(t) &= 6\Delta z_m(\omega t - \sin(\omega t)) \\ \Delta z(t) &= \Delta z_m(4 - 3\cos(\omega t)) \end{aligned} \tag{4.17}$$

  if the chaser is moving with the same velocity as the target.

For error assessments, both possibilities of a measurement error in the z-position must be taken into account as extreme cases, if the velocity measurement accuracy does not permit a clear distinction.

Example: Initial position measurement error in the z-direction of 10 m

If the chaser is moving on a parallel orbit:

- the position uncertainty in the x-direction according to Eqs. (3.25) after one orbital revolution is 94.25 m;
- the uncertainty in the velocity V_x according to Eq. (3.24) will be 0.01 m/s after one orbital revolution;

If the chaser is moving with the same velocity as the target:

- the uncertainty in the z-direction will be a maximum of 70 m after half an orbital revolution;
- the uncertainty in the x-direction is 370 m after one revolution.

To assess the potential error ellipsoid along the trajectory, the worst values of both cases would have to be considered, if the actual velocity cannot be measured with sufficient accuracy.

Velocity measurement errors

The effects of velocity measurement errors are the same as those of an initial velocity in a certain direction. Trajectory deviations due to velocity errors in the x-direction follow from Eq. (3.28) due to velocity errors in the y-direction from Eq. (3.40) and due to velocity errors in the z-direction from Eq. (3.34). The position errors are a linear function of the velocity error.

- Measurement error $\Delta V_{xm} \Longrightarrow$ trajectory errors of

$$\begin{aligned} \Delta x(t) &= \Delta V_{x\mathrm{m}} \left(\frac{4}{\omega} \sin(\omega t) - 3t \right) \\ \Delta z(t) &= \frac{2}{\omega} \Delta V_{x\mathrm{m}} (\cos(\omega t) - 1) \end{aligned} \tag{4.18}$$

- Measurement error $\Delta V_{y\mathrm{m}} \Longrightarrow$ trajectory error of

$$\Delta y(t) = \frac{1}{\omega} \Delta V_{y\mathrm{m}} \sin(\omega t) \tag{4.19}$$

- Measurement error $\Delta V_{z\mathrm{m}} \Longrightarrow$ trajectory errors of

$$\begin{aligned} \Delta x(t) &= \frac{2}{\omega} \Delta V_{z\mathrm{m}} (1 - \cos(\omega t)) \\ \Delta z(t) &= \frac{1}{\omega} \Delta V_{z\mathrm{m}} \sin(\omega t) \end{aligned} \tag{4.20}$$

For the following examples a 400 km orbit is assumed.

Example: Velocity measurement error in the x-direction

The position error will evolve according to the trajectory type shown in figure 3.15 for a ΔV in the x-direction. A velocity measurement error of 0.01 m/s in the x-direction results in a position error in the x-direction of 166 m per orbit and in a maximum of the position error in the z-direction (double amplitude) of 35 m after half an orbit.

Example: Velocity measurement error in the z-direction

The position error will evolve according to the trajectory type shown in figure 3.20 for a ΔV in the z-direction. A velocity measurement error of 0.01 m/s in the z-direction results in a maximum of the position error in the x-direction of 35 m after half an orbit and in an amplitude of the position error in the z-direction of 8.8 m after one quarter orbit.

Example: Velocity measurement error in the y-direction

The position error will evolve according to the trajectory type shown in figure 3.23 for a ΔV in the y-direction. A velocity measurement error of 0.01 m/s in the y-direction results in an amplitude of the position error in the y-direction of 8.8 m after one quarter orbit.

Attitude and angular rate measurement errors

Attitude errors have no direct effect on the trajectory evolution. However, they do have an effect on the trajectory during boost manoeuvres, as they result in undesirable components of the thrust in directions other than the intended ones. This case is treated in section 4.3.2 under 'thrust direction errors'.

Angular rates have no direct effect on the trajectory evolution, except for the attitude achieved at the boost manoeuvre (see above).

4.3.2 Trajectory deviations due to thrust errors

Thrust errors can be caused by errors in the magnitude of the thrust force (ΔF), in the actual mass of the spacecraft (Δm), in the thrust duration (Δt) and in the thrust direction ($\Delta \alpha$) w.r.t. the values assumed in the calculation. These errors can be due to mounting errors, to misalignments of the exhaust flow velocity vector w.r.t. the mechanical axis of the nozzle, to impingement of the thrust plumes on the structure of the own spacecraft, to deviation of the actual specific impulse from the nominal one, to non-linearities of the delivered ΔV w.r.t the valve opening time, etc.

Thrust force and duration errors

The applied thrust force per unit mass is

$$\gamma_{\mathrm{t}} = \frac{F_{\mathrm{t}}}{m_{\mathrm{c}}}$$

where F_{t} is the nominal thrust force and m_{c} is the mass of the spacecraft. The actual thrust force per unit mass including errors can be defined as

$$\begin{aligned} \gamma &= \gamma_{\mathrm{t}} + \Delta\gamma \\ \gamma &= \gamma_{\mathrm{t}}\, \epsilon_\gamma \end{aligned}$$

where γ_{t} is the nominal thrust force/mass and ϵ_γ is the thrust error factor,

$$\epsilon_\gamma = 1 + \frac{\Delta\gamma}{\gamma_t}$$

If the thrust error is due to the assumed thrust force level, then

$$\epsilon_\gamma = 1 + \frac{\Delta F}{F_{\mathrm{t}}}$$

If the thrust error is due to an error of the assumed mass, then

$$\epsilon_\gamma = 1 + \frac{m_{\mathrm{c}}}{\Delta m}$$

The actual duration of the thrust, including errors, can be defined as

$$\begin{aligned} t &= t_{\mathrm{t}} + \Delta t \\ t &= t_{\mathrm{t}}\, \epsilon_{\mathrm{t}} \end{aligned}$$

where t_{t} is the nominal thrust duration and ϵ_{t} is the duration error factor,

$$\epsilon_t = 1 + \frac{\Delta t}{t_t}$$

Resulting position and velocity errors

The actual position x_{act} and the actual velocity $\dot{x}_{\mathrm{act}}$ may be similarly defined:

$$\begin{aligned} x_{\mathrm{act}}(t) &= x_{\mathrm{th}} + \Delta x \\ x_{\mathrm{act}}(t) &= x_{\mathrm{th}}\, \epsilon_x \end{aligned}$$

where x_{th} is the nominal x-component and $\epsilon_x =$ trajectory error factor,

$$\epsilon_x = 1 + \frac{\Delta x}{x_{\mathrm{th}}}$$

and

$$\begin{aligned} \dot{x}_{\mathrm{act}}(t) &= \dot{x}_{\mathrm{th}} + \Delta\dot{x} \\ \dot{x}_{\mathrm{act}}(t) &= \dot{x}_{\mathrm{th}}\, \epsilon_{Vx} \end{aligned}$$

where $\dot{x}_{\rm th}$ is the nominal x-component and ϵ_{Vx} is the velocity error factor,

$$\epsilon_{Vx} = 1 + \frac{\Delta\dot{x}}{\dot{x}_{\rm th}}$$

(correspondingly for y, z, $\dot{y}$, $\dot{z}$).

Using the above relations, the equations of motion for continuous thrust manoeuvres with deviations due to thrust errors become as follows.

Thrust in the x-direction The actual trajectory with thrust errors ($x_{\rm th}$, $z_{\rm th}$ from Eq. (3.59)) is

$$\begin{aligned} x_{\rm act}(t) = x_{\rm th}(t)\,\epsilon_x &= \gamma_x\epsilon_\gamma\left(\frac{4}{\omega^2}(1-\cos(\omega t_{\rm t}\epsilon_{\rm t})) - \frac{3}{2}t_{\rm t}^2\epsilon_{\rm t}^2\right) \\ z_{\rm act}(t) = z_{\rm th}(t)\,\epsilon_z &= \frac{2}{\omega^2}\gamma_x\epsilon_\gamma(\sin(\omega t\epsilon_{\rm t}) - \omega t\epsilon_{\rm t}) \end{aligned} \tag{4.21}$$

The actual velocities with thrust errors ($\dot{x}_{\rm th}$, $\dot{z}_{\rm th}$ from Eq. (3.60)) are

$$\begin{aligned} \dot{x}_{\rm act}(t) = \dot{x}_{\rm th}(t)\,\epsilon_{Vx} &= \gamma_x\epsilon_\gamma\left(\frac{4}{\omega}\sin(\omega t\epsilon_{\rm t}) - 3t\epsilon_{\rm t}\right) \\ \dot{z}_{\rm act}(t) = \dot{z}_{\rm th}(t)\,\epsilon_{Vz} &= \frac{2}{\omega}\gamma_x\epsilon_\gamma\left(\cos(\omega t\epsilon_{\rm t}) - 1\right) \end{aligned} \tag{4.22}$$

Thrust in the y-direction The actual trajectory with thrust errors ($y_{\rm th}$ from Eq. (3.75)) is

$$y_{\rm act}(t) = y_{\rm th}(t)\,\epsilon_y = \frac{1}{\omega^2}\gamma_y\epsilon_\gamma(1-\cos(\omega t\epsilon_{\rm t})) \tag{4.23}$$

The actual velocities with thrust errors ($\dot{y}_{\rm th}$ from Eq. (3.76)) are

$$\dot{y}_{\rm act}(t) = \dot{y}_{\rm th}(t)\,\epsilon_{Vy} = \frac{1}{\omega}\gamma_y\epsilon_\gamma\sin(\omega t\epsilon_{\rm t}) \tag{4.24}$$

Thrust in the z-direction The actual trajectory with thrust errors ($x_{\rm th}$, $z_{\rm th}$ from Eq. (3.66)) is

$$\begin{aligned} x_{\rm act}(t) = x_{\rm th}(t)\,\epsilon_x &= \frac{2}{\omega^2}\gamma_z\epsilon_\gamma(\omega t\epsilon_{\rm t} - \sin(\omega t\epsilon_{\rm t})) \\ z_{\rm act}(t) = z_{\rm th}(t)\,\epsilon_z &= \frac{1}{\omega^2}\gamma_z\epsilon_\gamma(1-\cos(\omega t\epsilon_{\rm t})) \end{aligned} \tag{4.25}$$

The actual velocities with thrust errors ($\dot{x}_{\rm th}$, $\dot{z}_{\rm th}$ from Eq. (3.67)) are

$$\begin{aligned} \dot{x}_{\rm act}(t) = \dot{x}_{\rm th}(t)\,\epsilon_{Vx} &= \frac{2}{\omega}\gamma_z\epsilon_\gamma\left(1-\cos(\omega t\epsilon_{\rm t})\right) \\ \dot{z}_{\rm act}(t) = \dot{z}_{\rm th}(t)\,\epsilon_{Vz} &= \frac{1}{\omega}\gamma_z\epsilon_\gamma\sin(\omega t\epsilon_{\rm t}) \end{aligned} \tag{4.26}$$

From the above equations it follows immediately that errors in the applied force per unit mass lead to directly proportional errors in trajectory and velocity. Errors in thrust duration, on the other hand, repercuss on the development of trajectory and velocities via the more complex time dependent terms in the above equations.

Thrust duration errors are for all nominal operations very small, as time can be measured very accurately and delays due to valve operations are low. Nevertheless, there is one case where thrust duration errors are important, i.e. in the case of 'thruster-open' failures. In such cases, the failure condition can be detected usually only by observation of secondary effects, such as temperature and pressure in the thruster, saturation of control commands, state vector deviations, etc. Detection of 'thruster-open' failure may, therefore, take some time, during which thrust continues to the full extent.

Examples

In the following examples only the position and velocity errors due to thrust duration errors are considered. The absolute values of γ and ω do not play a role as they are identical for the actual and theoretical values. The position and velocity errors are, according to Eqs. (4.21)–(4.26), a function of time. The examples have been calculated for a nominal thrust duration of 10% of the orbital revolution ($\approx$ 550 s in a 400 km orbit) and a thrust duration error of 5% . At the end of the thrust the trajectory and velocity errors are as follows:

X-thrust	$\epsilon_x = 1.086$ (8.6 % error)	$\epsilon_{Vx} = 1.014$ (1.4 % error)
	$\epsilon_z = 1.155$ (15.5 % error)	$\epsilon_{Vz} = 1.099$ (9.9 % error)
Y-thrust	$\epsilon_y = 1.099$ ((9.9 % error)	$\epsilon_{Vy} = 1.043$ (4.3 % error)
Z-thrust	$\epsilon_x = 1.155$ (15.5 % error)	$\epsilon_{Vx} = 1.099$ (9.9 % error)
	$\epsilon_z = 1.099$ (9.9 % error)	$\epsilon_{Vz} = 1.043$ (4.3 % error)

A thrust duration for a single manoeuvre of one tenth of an orbital revolution ($\approx$ 9 min) is very long and a duration error of 5% (27 s) is of course, even for detection of thruster failures, very high. These values have been chosen simply to demonstrate the effects. For thrust durations which are fractions of one orbital revolution, the errors will of course be different. The example shows, however, that the relative trajectory and velocity errors may, depending on the direction of thrust, be much higher than the relative duration error.

Thrust direction errors

Thrust direction errors can be caused by the attitude error of the vehicle w.r.t. the orbital frame, by geometric misalignment of the thruster hardware, or by a misalignment of the thrust vector w.r.t. the centre line of the thruster nozzle. This latter may be caused by flow-dynamic asymmetries. As in the case of attitude measurement errors, thrust direction errors lead to a component of thrust in a perpendicular direction.

Example

For a ΔV of 1 m/s, an attitude error of 1 deg results in an undesired component in a perpendicular direction of 0.0175 m/s, with the effects described above under 'Resulting position velocity errors'. For an impulsive manoeuvre in a 400 km orbit, e.g., the position error in the *x*-direction would be approximately 290 m per orbit, and the amplitude in the *z*-direction would be about 31 m.

For finite thrust manoeuvres, the direction of the applied force vector has to be taken into account:

$$\Delta\gamma_{\perp} = \gamma_{\mathrm{t}} \sin \Delta\alpha_{\mathrm{t}} \tag{4.27}$$

where $\Delta\alpha_{\mathrm{t}}$ is the direction error.

Depending on the original thrust direction and on the direction of the error angle, the corresponding trajectory and velocity errors in a perpendicular direction can be obtained by inserting the value found for $\Delta\gamma_{\mathrm{t}}$ into Eqs. (3.59)–(3.76), as in the previous cases.

4.3.3 Trajectory deviations due to thruster failures

Under the term 'thruster failure', as explained in section 4.1.3, two failure conditions are understood; these correspond to the inability to close the thruster valves at the end of operation (*thruster-open failure*) and to the inability to open the valves for operation (*thruster-closed failure*). Other failure conditions, where a thruster permanently produces a partial thrust level, are qualitatively equivalent to a thruster-open failure.

Thruster-open failure

A rendezvous vehicle must have the capability of producing control forces in all directions and will have an according combination of thrusters. Depending on the direction of the failed thruster, thruster-open failures, if not counteracted in time, can lead to any type of trajectory. The magnitude of the eventual trajectory and velocity errors depends on the duration of the failure condition. As a result, there is no other protection against thruster-open failures but to detect this failure condition as early as possible and to stop the thrust force (see section 4.4.1). The residual maximum possible trajectory and velocity errors can then be calculated from the worst case time difference between failure occurrence and closure of the faulty thruster (see the remark about thrust duration errors in section 4.3.2).

Thruster-closed failure

Thruster-closed failures, if no more redundancy is available and if not resolved in time, lead to loss of attitude control around one axis and loss of trajectory control in one direction. A resulting uncontrolled angular motion about this axis may, after time, cause a coupling of trajectory control forces from one axis in the others, resulting in trajectory deviations. The effects of an unresolved thruster-closed failure are, in the short term,

the inability to perform a planned trajectory manoeuvre and, in the longer term, the loss of attitude and the build-up of trajectory deviations. If the failed thruster can be identified, and as long as redundancy is available, the obvious solution is to inhibit the failed thruster and to switch over to a redundant one. Otherwise, a certain protection against the long term effects of thruster-closed failures concerning the collision with the target spacecraft would be the inhibition of all thrusters, provided the resulting trajectory would be collision-free (see section 4.4.2).

4.4 Protection against trajectory deviations

According to the failure tolerance requirements and design rules discussed in section 4.1.1, the trajectory strategy has to be designed such that if, due to errors and failures, the planned trajectory cannot be maintained, the resulting motion of the chaser vehicle will not lead to collision with the target. To ensure adherence to the planned trajectory, considering the various causes of trajectory deviations and the possibility of thruster failures as discussed above, the active detection and correction of trajectory deviations is the sole option (*active trajectory protection*). If it is no longer possible, for whatever reasons, to maintain this active protection, it must be attempted to keep the vehicle on a 'safe trajectory', i.e. a trajectory which remains collision-free when all thrust is inhibited (*passive trajectory protection*). This would also be the ultimate protection of the target vehicle against collision in the case of a complete loss of all control functions (examples would be the complete loss of power, an explosion or (e.g.) damage by meteorite or debris impact). However, not all parts of the approach trajectory sequence can be protected in this way. When the approaching vehicle is in very close proximity to the target, trajectories are designed 'to make contact', whether directly with a particular location on the target geometry (docking), or with a virtual 'reception box' in the very close vicinity (berthing). In such cases only an active *collision avoidance manoeuvre* (CAM) by the chaser can provide the required protection of the target vehicle. It should be pointed out that there are limitations concerning the range down to which a CAM can be defined. These may be given on one hand by the distance required for braking and on the other hand by thermal loads and contamination of the target surface due to the thruster plume of the CAM. As a result, a CAM cannot be used during the last metre prior to contact.

4.4.1 Active trajectory protection

Active trajectory protection requires the detection and correction in time of trajectory deviations. This principle of closed loop detection and correction is already applied in practically all spacecraft for attitude control. Another convenient solution to the problem of the control of trajectory deviations would be for the evolution of the trajectory to be closed loop controlled. Such active control is usually performed for forced trajectories, such as straight line V-bar and R-bar approaches and manoeuvres. This principle

can also be applied, however, to free drift and impulsive trajectories. In these cases the evolution of the nominal trajectory and velocities over time will be pre-calculated and closed loop controlled within narrow margins (controlled nominal trajectory scheme). As attitude and angular rate will also be closed loop controlled, the control of the spacecraft's state vector would comprise the control of a total of 12 values, i.e. three positions, three velocities, three angles and three angular rates. For two-pulse manoeuvres, the

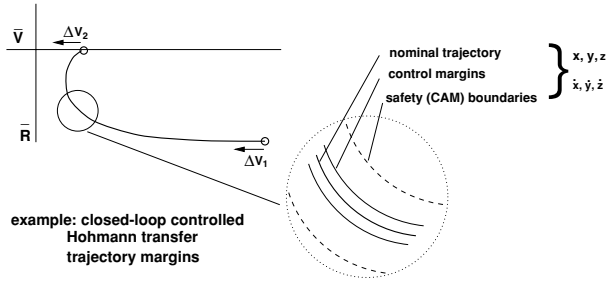

Figure 4.8. Example of the monitoring of safety of state vector: Hohmann transfer.

boost phases of the transfer can also be closed loop controlled. In this case the boosts are entered as feed-forward commands into the control loop by the guidance function (see chapter 7), while the controller minimises the control error w.r.t. the pre-calculated nominal trajectory. In order to keep the control effort small, known disturbances such as differential drag can be included in the calculation of the 'nominal' trajectory, where by nominal we mean 'to the extent known'.

Other methods of trajectory protection for free drift and impulsive manoeuvres include the application of one or more 'mid-course manoeuvres', where corrective ΔVs will be applied to achieve the intended final position. Compared with the continuous control of the nominal trajectory, a scheme with a few mid-course correction manoeuvres will of course result in a lower propellant consumption, which is why it is often preferred to the 'continuous nominal trajectory control scheme'.

A special case of this 'mid-course manoeuvre' strategy is the 'continuous targeting scheme', where the final position is continuously closed loop controlled, i.e. for each control cycle the ΔVs to reach this point are calculated from the instantaneous position, velocities and time.

During the rendezvous phase, i.e. in proximity of the target, the two latter schemes must be considered less safe than the 'controlled nominal trajectory scheme', as only the final position is actively controlled rather than the state vector at each point of the trajectory. In case of failure of the control system, all state vector values are, at the instance of failure, for the 'controlled nominal trajectory scheme' still nominal, whereas, for the 'continuous targeting scheme' the deviation of the actual from the nominal state vector values is uncontrolled. This can have repercussions on the validity of the passive trajectory protection concept (see the following section), the concept of which is based

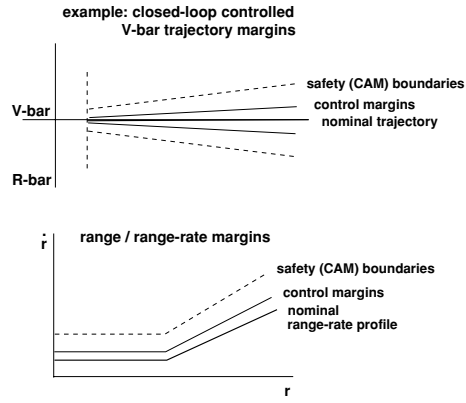

Figure 4.9. Example of monitoring of safety of state vector: V-bar approach.

on the nominal evolution of trajectories plus certain margins.

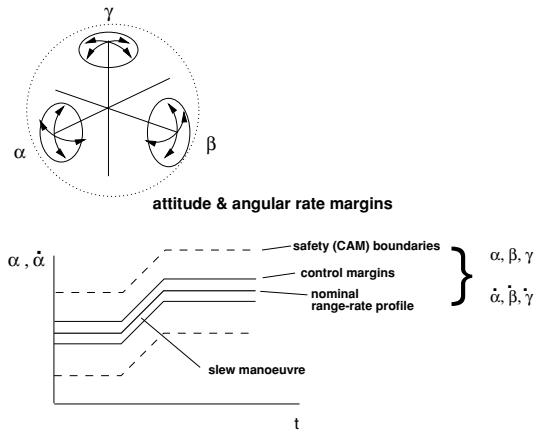

Figure 4.10. Monitoring of safety of state vector, attitude and attitude rate.

Closed loop control of a nominal trajectory also allows easy implementation of criteria for the initiation of a CAM. If the pre-calculated boundaries of safety margins around the nominal state vector values have been reached, the trajectory will be judged 'unsafe' (whether by the onboard system or by human observers) and a CAM will be commanded. For other schemes, safety criteria for position and velocities are more difficult to establish, and, in the case of the 'continuous targeting scheme', would have to be re-calculated continuously. Figures 4.8, 4.9 and 4.10 show schematically the con-

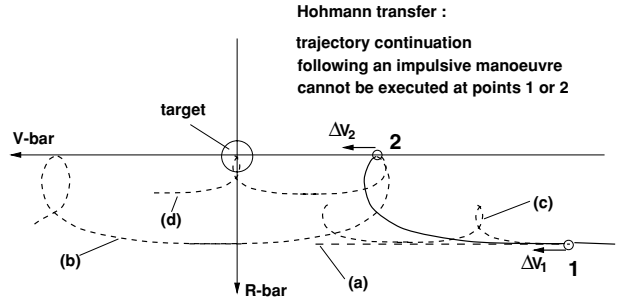

Figure 4.11. Passively safe trajectories: Hohmann transfer.

trol margins and safety boundaries for an impulsive transfer trajectory for a straight line V-bar approach with velocity profile and for attitude control.

Other important trajectory elements of the rendezvous phase, which require closed loop control and safety boundary monitoring, are hold points. If not actively controlled, a drift motion as shown in figure 4.3 will commence. Active trajectory protection requires sufficiently accurate navigation information on all state vector values throughout the entire duration of the trajectory element.

4.4.2 Passive trajectory protection

The basic idea of passive trajectory protection is, as stated above, to design all trajectory elements in an approach trajectory sequence such that if, at any point of the trajectory, thrust control ceases, the resulting 'free trajectory' will remain collision-free for TBD time. Such a property would not only be protection against the case of total disablement of the approaching vehicle, but would also allow the implementation of a straightforward and effective way of achieving collision safety by simply commanding the thrust to stop. Actually, a complete inhibition of thrust may often be the sole possible immediate action after thruster-open failures and malfunction of the control system, as long as the failure source has not been identified. This concept, of course, will not work in the very close vicinity of the target. Eventually the chaser vehicle will be so close that actual limits are determined by the geometric extensions of the two vehicles and by the absolute value and control margins of their motion. Unfortunately also prior to this closest range for passive trajectory safety, thrust failures can cause trajectory evolutions, which may lead to collision with the target. In the following, various types of trajectories will be analysed concerning their passive safety properties for thruster-closed failures (thruster-open failures must be dealt with by active means; see section 4.3.3). The examples shown in figures 4.11–4.14, are given for an approach on −V-bar. For an approach on +V-bar the trajectories have to be mirrored on both the V-bar and R-bar axes.

Hohmann transfer

The first type of trajectory to be analysed is the transfer to a different altitude by a two-pulse tangential thrust manoeuvre, i.e. a Hohmann transfer (figure 4.11). The first boost is to be applied at point 1 in the +V-bar direction, and the second, at point 2 after one half revolution, must be of the same magnitude and direction to stop the motion at the new z-position. To achieve the required ΔV, the available thrust force γ_x has to be applied during the nominal thrust time t (see the equations of motion (3.59)). The following failure cases have to be considered:

(1) When the first boost (ΔV_1 at point 1) cannot be executed, the trajectory continues as a free drift (trajectory (a)). This trajectory is safe w.r.t. collision.

(2) When the second boost (ΔV_2 at point 2) cannot be executed, the trajectory continues looping with an apogee at V-bar and a perigee at the z-distance of point 1 (trajectory (b)). The x-positions of point 1 and point 2 have to be chosen in such a way that the next following perigee will be near the x-location of the target and the next following apogee will be in front of the target. Under these conditions this trajectory is safe w.r.t. collision.

(3) When control ceases somewhere between the first and the second boost, the result is the same as for (2), i.e. trajectory (b).

(4) When the first boost is interrupted somewhere within its nominal duration, the motion in the x-direction up to the first apogee will be shorter, but also the z-position of the apogee will be lower (trajectory (c)). Only in cases involving a very large extension of the target geometry in the z-direction might there be a danger of collision. By adapting the position of point 1 accordingly, this can be avoided for each individual case. Under these conditions this trajectory is safe w.r.t. collision.

(5) When the second boost is interrupted somewhere within its nominal duration, the trajectory will not stop at point 2 but will continue with smaller loops with an apogee very near to V-bar and a perigee depending on the percentage of the planned second boost realised (trajectory d). In this case a very large region within the nominal duration of the second boost, where propulsion is stopped, could lead to collision with the target. This part of a Hohmann transfer cannot be rendered passively safe. The sole protection against a thruster-closed failure during the second boost is a CAM.

Tangential thrust transfer along V-bar

The second type of trajectory to be analysed here is a transfer along V-bar by two tangential boosts (figure 4.12). The first boost (thrust force γ_x over nominal thrust duration t, Eqs. (3.59)) to be applied in point 1 is in the −V-bar direction, and the second, at point

2 after one orbital revolution, is of the same magnitude but in the opposite direction to stop the motion at the new x-position.

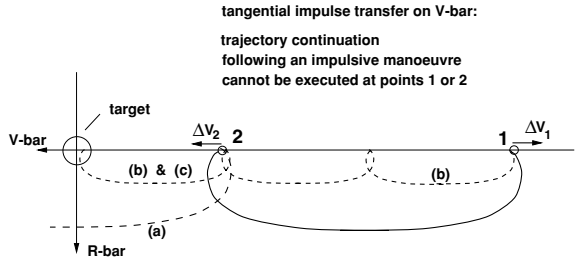

Figure 4.12. Passively safe trajectories: tangential boost transfer.

The following failure cases have to be considered:

(1) When the first boost at point 1 cannot be performed, the vehicle remains at that point. This condition is safe (for the influence of differential drag see below).

(2) When the second boost (ΔV_2 at point 2) cannot be executed, the trajectory continues looping with an apogee at V-bar and a perigee at the z-distance of point 1 (trajectory (a)). This situation is very similar to the case of the Hohmann transfer, discussed in the first example. The x-positions of point 1 and point 2 have to be chosen in such a way that the next following perigee will be near the x-location of the target and the next following apogee will be in front of the target. Under these conditions this trajectory is safe w.r.t. collision.

(3) When control ceases somewhere between the first and the second boost, the result is the same as for (2), i.e. trajectory (a).

(4) When the first boost is interrupted somewhere within its nominal duration, the trajectory will start with smaller loops, with an apogee at V-bar and a perigee depending on the percentage of the planned first boost that has been realised (trajectory (b)). For a propulsion failure which cannot be resolved within one orbital revolution, the trajectory continues looping, with a large chance that at one of the following apogees the target is hit, or that the perigee is of the same order of magnitude as the extension of the target geometry in the z-direction and the target will be hit in any case. This case is unsafe. The sole protection against a thruster-closed failure during the first boost of the tangential thrust V-bar transfer is a CAM.

(5) When the second boost is interrupted somewhere within its nominal duration, the situation is identical to the previous one: the trajectory continues looping, with a large chance that the target is hit at one of the following apogees, or that the

perigee distance is so small that the target will be hit anyway (trajectory (c)). Again, the sole protection is a CAM.

The analysis shows that the tangential thrust transfer on V-bar has relatively bad passive safety properties, as a thruster-closed failure at partial burns (of both burns) can lead to collision. The tangential thrust type of trajectory is, for this reason, less suitable as the trajectory element for close range approach. For other purposes, however, this trajectory may have advantages w.r.t. ground station visibility (communication window) and illumination conditions. Due to its transfer time of one orbit, such conditions may be equal or similar in the following revolution.

Radial thrust transfer along V-bar

The third type of trajectory to be analysed for passive safety is the transfer on V-bar by radial impulses, as shown in figure 4.13. The first boost (thrust force γ_z over nominal thrust time t, Eqs. (3.66)) is to be applied at point 1 in the +R-bar direction, and the second, at point 2 after one half orbital revolution, has to be of the same magnitude and direction.

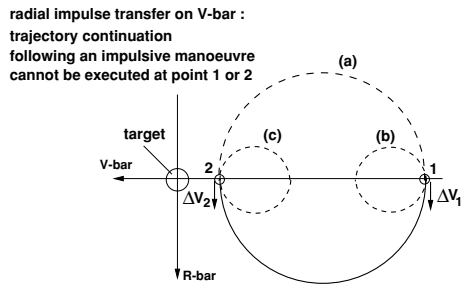

Figure 4.13. Passively safe trajectories: radial boost transfer.

The following failure cases have to be considered:

(1) When the first boost at point 1 cannot be performed, the vehicle remains at that point. This condition is safe (for the influence of differential drag see below).

(2) When the second boost at point 2 cannot be performed, the trajectory will return after each orbit, if no disturbance forces are acting, to the starting point 1 (trajectory (a)). This trajectory is safe w.r.t. collision in the short term. This also means that under the influence of differential drag the trajectory will not hit the target for at least one orbital revolution or more, the number of revolutions depending on the ratio of ballistic coefficients of the two vehicles and on the distance between point 2 and the target.
If the ratio of the ballistic coefficients of chaser and target is such that an average motion toward the target would result, an additional small tangential boost in

the $+x$-direction can be applied at point 1 to ensure that the trajectory will, on average, move away from the target, at least for a number of orbital revolutions.

(3) When control ceases somewhere between the first and the second boost, the result is the same as for (2), i.e. trajectory (a).

(4) When the first boost is interrupted somewhere within its nominal duration, the motion in the x-direction up to the first return to V-bar will, depending on the percentage of the planned first boost that has been realised, be shorter, and the trajectory will, if not stopped, loop between this point and point 1 (trajectory (b)). The trajectory is safe in the same way as in failure case (1), except that the shortest distance to the target is larger.

(5) When the second boost is interrupted somewhere within its nominal duration, the trajectory will loop back after half an orbit to a point on V-bar between point 1 and point 2, depending on the percentage of the planned second boost that has been realised. It would return without drag after each following revolution to point 2. The trajectory is safe in the same way as in failure case (1).

Straight line V-bar and R-bar approaches

The next class of trajectories to be analysed comprises the straight line forced motion trajectories used for V-bar and R-bar final approaches to the docking port or to a berthing position at the target. These types of trajectories (see section 3.3.3) require the continuous application of thrust to counteract the Coriolis forces. If these thrust forces are stopped, the resulting trajectories are as shown in figures 3.13 and 3.14.

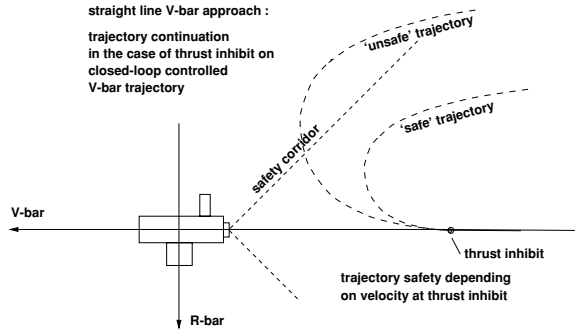

Figure 4.14. Passively safe trajectories: V-bar approach.

The passive safety of these trajectories depends on the approach velocity and on the distance from the docking port of the target. The trajectory can be kept safe by reducing the velocity according to the distance from the target. However, as (a) the target has a geometric extension in the $+$ and $-z$-directions, (b) trajectory and velocity control

margins have to be taken into account and (c) in the case of docking a final velocity has to be maintained, the last part of a straight line final approach trajectory cannot be made passively safe in this way. In addition, safety corridors may have to be observed (see also section 5.6). The situation w.r.t. safety corridors of free drift trajectories after inhibiting thrust forces is shown schematically in figure 4.14. For all these practical reasons, in the last 100 m of the approach passive trajectory safety cannot be relied on, and the sole protection, when active trajectory control has failed, is a CAM.

Long term trajectory safety

In the above discussion of the various trajectories concerning passive trajectory safety, no trajectory disturbance forces have been considered, and it was sufficient, for assessing trajectory safety, to look at the trajectory evolution for only one or very few orbital revolutions. However, as in reality drag forces are always present, the obtained results can be valid only for a short time. In the example shown in figure 4.15, where the trajectory starts with a tangential impulse of $\Delta V = 0.06$ m/s, it returns after about ten orbital revolutions to its origin. In this example an average density of 9.4×10^{-12} $\mathrm{km/m^3}$ has been assumed, which is similar to that assumed for the examples shown in figures 4.2–4.5. The ballistic coefficient of the chaser is again $C_{\mathrm{BC}} = 470$ kg/m^2 and the ratio of the ballistic coefficients of chaser and target is assumed to be $C_{\mathrm{Bc}}/C_{\mathrm{Bt}} = 5$. The direction and magnitude of the long term effect of the differential drag on the

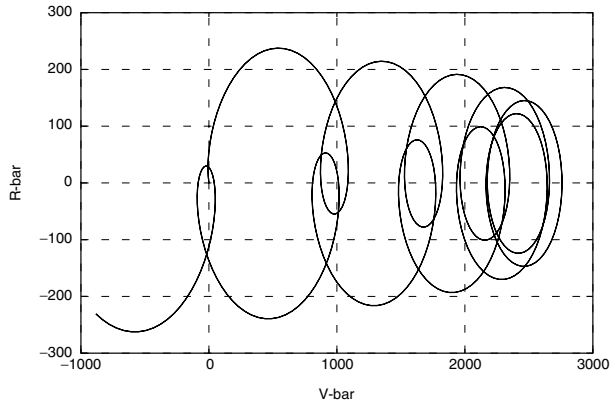

Figure 4.15. Tangential impulse −0.06 m/s with differential drag (400 km orbit).

trajectory development of the chaser depends, of course, on the value of $C_{\mathrm{Bc}}/C_{\mathrm{Bt}}$ (see Eq. (4.3)), as already shown in figures 4.3–4.5. Because of the differential drag effects, the approach from the −V-bar side is generally safer for a chaser with a higher C_{B} (and vice versa).

4.5 Collision avoidance manoeuvres

It has been identified above that the execution of a CAM will become necessary when active trajectory control has failed and when the present trajectory, or the present part of it, is not passively safe. Failure of active trajectory control can be caused by a number of reasons, e.g. by sensors, thrusters, GNC functional problems, software problems, etc. Such failures can be identified either on the level of the hardware and software functions involved in the process, or, e.g., by detection of violation of the safety margins of the various nominal state vector values, as discussed above (see also section 6.4).

Detection of contingencies due to violation of safety margins and corridors or due to loss of functions may be performed both by the onboard system and by remote human operators in the target spacecraft or on ground (see also section 9.1.2). After detection of a contingency case, a scheme for recovery could consist of the following steps:

(1) Switch to the redundant single equipment if the faulty equipment can be identified.

(2) Switch to the redundant string if the failure cannot be isolated. This includes switching to a redundant processor with identical rendezvous control software.

(3) If problems cannot be solved by redundancy switching, and the danger of collision still exists, either execute a CAM or inhibit trajectory control actuation, to leave the vehicle on a safe drift trajectory (if available).

In order to fulfil the failure tolerance requirements discussed in sections 4.1.1 and 4.1.2, the onboard system for rendezvous control and its constituents must of course provide sufficient redundancy. For essential equipment, such as data management equipment, reaction control system hardware, gyros, etc., double redundancy must be available.

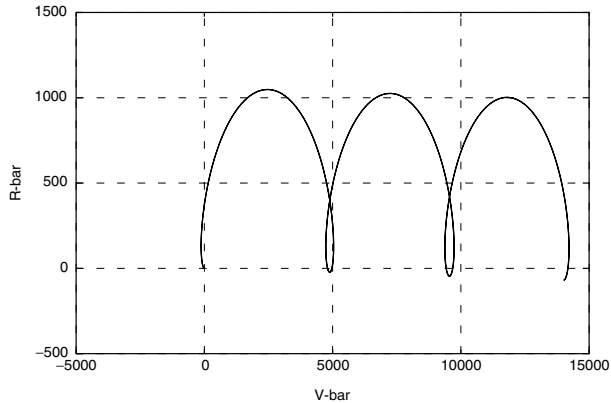

Figure 4.16. CAM on −V-bar: 0.3 m/s $-x$-boost, influence of differential drag.

As a collision avoidance manoeuvre must still function when the GNC system has failed or is malfunctioning, such a manoeuvre must be as simple as possible and be executable with a minimum of onboard resources. The simplest case is a single boost in the opposite approach direction. As such a manoeuvre is not very sensitive to the attitude (even at an attitude error of 15 deg, the cosine is still 0.966, i.e. the reduction in thrust is less than 4%), the thrust manoeuvre can be assigned to a fixed direction in the spacecraft geometric frame $\boldsymbol{F}_{\mathbf{ge}}$ instead of the local orbital frame $\boldsymbol{F}_{\mathbf{lo}}$. Then, no functioning onboard GNC system is required, since the operation consists only of addressing the specific thrusters and opening the thruster valves for a fixed time period.

An example of a CAM for a $-$V-bar approach is shown in figure 4.16. The CAM consists of an application of a ΔV in the $-x$-direction. The drag conditions are assumed to be the same as in figure 4.15, i.e. the average density is $9.4 \times 10^{-12}\ \mathrm{km/m^3}$ and the ratio of ballistic coefficients is $C_{\mathrm{Bc}}/C_{\mathrm{Bt}} = 5$. The boost is five times as strong as in figure 4.15, and the relative influence of differential drag is accordingly lower. For an approach on $+$V-bar, the same type of manoeuvre in the $+x$-direction would be applied, with the resulting trajectory mirrored on the x- and z-axes.

The amount of ΔV to be applied for a CAM depends on (a) the geometric extension of the target in the z-direction, (b) the relative velocity the chaser has at CAM initiation (or the maximum velocity of the trajectory element for which the CAM shall be valid) and (c) the time for which the CAM trajectory must be guaranteed collision-free. The primary requirement, i.e. to render the escape trajectory collision-free over the next few orbits, can be fulfilled with relatively small ΔVs. For very large chaser to target C_{B} ratios of 5–10, and for guaranteed collision protection over a long duration, such as 24 h, ΔVs of more than 1 m/s may be required for a V-bar CAM.

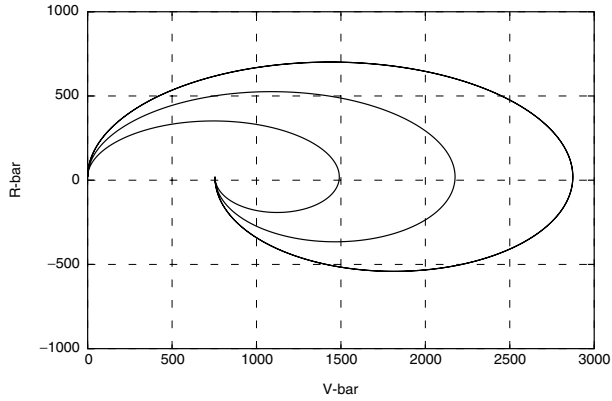

Figure 4.17. CAM on R-bar: $\Delta V_z = 0.3,\ 0.5,\ 0.7$ m/s, z = 20 m (one orbit).

For CAM on R-bar the situation is less simple. If the CAM were to consist of an application of a ΔV in the z-direction, the advance in the x-direction would depend

only on the z-position, where the CAM is applied. The resulting motion is obtained by addition of the equation for the release at a z-position moving with the velocity of the target (Eqs. (3.25)) and of the equation for a radial ΔV, Eqs. (3.34). As the latter equation does not include an average advance over one orbit, the average motion in the x-direction is only due to the z-distance of the CAM initiation point from the target orbit. This is shown clearly by the examples in figures 4.17 and 4.18. In figure 4.17, the CAM trajectory starts at 20 m, and three values for the radial ΔV have been assumed: 0.3 m/s, 0.5 m/s and 0.7 m/s. Figure 4.17 shows that the undisturbed trajectories all end, after one revolution, at the same point. In figure 4.18, the same ΔV is applied for all trajectories, but the initiation points are different, i.e. 20 m, 50 m and 100 m below the target orbit. This figure shows that the x-position after one revolution is strongly dependent on the z-position.

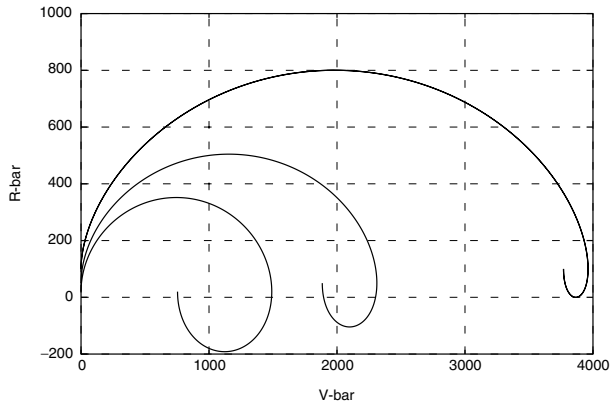

Figure 4.18. CAM on R-bar: $\Delta V_z = 0.3$ m/s, $z = 20$, 50, 100 m (one orbit).

A pure radial ΔV will, therefore, not be sufficient when the chaser vehicle is very close to the target. When the distance to the target orbit becomes only a few metres, the net advance after one revolution may be less than the diameter of a safety zone defined around the target (see section 5.6). An additional ΔV in the $-x$-direction could provide in this case the required advance in the orbital direction. The initial direction of the trajectory resulting from this combined x- and z-boost will, however, not necessarily be aligned with the approach axis. If there are elements of the target structure around the R-bar docking port or berthing box (see section 5.3), the ratio of $\Delta V_x/\Delta V_z$ must be chosen carefully to ensure that the escape trajectory will remain within the volume available for departure, including all dispersion and geometric extensions and margins of chaser and target.

An example of a CAM at the end of an R-bar approach at 15 m below the target orbit is shown in figures 4.19 and 4.20. The ratio of the ΔVs in the z- and x-directions

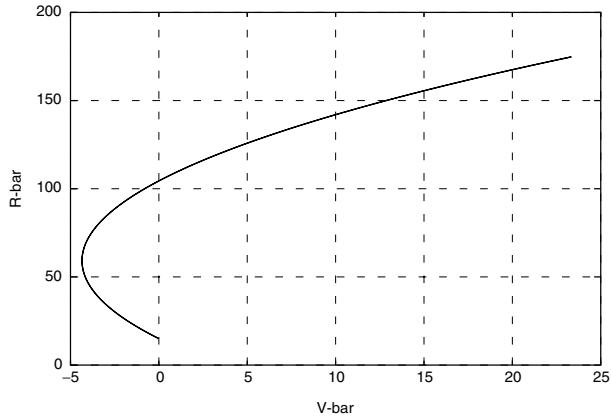

Figure 4.19. Example. CAM on R-bar: $\Delta V_z = 0.5$ m/s, $\Delta V_x = -0.1$ m/s (5 min).

is 5:1. Figure 4.19 shows that the trajectory in the first minutes will safely move below potential structural elements of the target. Figure 4.20 (same dynamic conditions) shows that after one orbital revolution the chaser will end up at a distance of more than 2000 m in front of the target.

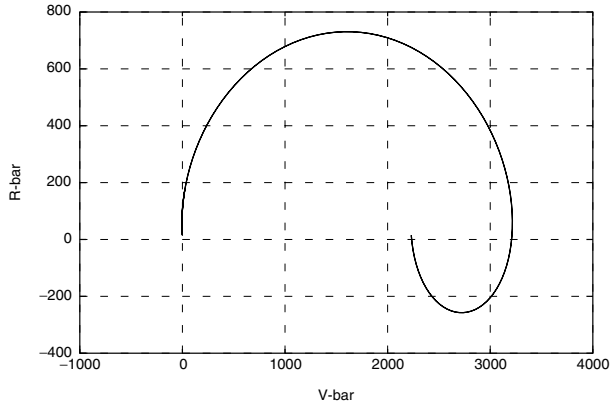

Figure 4.20. Example. CAM on R-bar: $\Delta V_z = 0.5m/s$, $\Delta V_x = -0.1$ m/s (one orbit).

Other important considerations which should be taken into account for the definition of the ΔV for a CAM are the time and propellant for recovery. The larger the CAM, the more time it will take for recovery, and consequently other resources of the vehicle have to be taken into account, in particular power. For the majority of the cases the time between the occurrence of a failure and the potential collision with the target is relatively long (from a couple of minutes up to one or more orbital revolutions), and therefore it

is very important that the human operators on ground or in the target station have other means at their disposal to stop or re-direct the motion of the spacecraft and to recover the mission (see chapter 9).

A CAM is the last resort in achieving safety against collision, which must still be available even after two failures, e.g. when the GNC system is no longer available. An open loop CAM requires that the attitude of the vehicle at initiation and during execution is approximately in the nominal direction. We have seen above that an attitude error of ± 15 deg is still not critical. However, as a failure situation which requires a CAM may also lead to uncontrolled angular rates, and as the achievement of a certain ΔV will take some time according to the mass of the vehicle and the size of the thrusters, there will be limitations to the application of open loop CAM manoeuvres.

In the case of a contingency situation, it must be possible for a CAM to be initiated both automatically by the onboard system according to certain failure criteria (see section 6.4), and directly by remote operators. However, as a CAM can endanger mission success and might not be absolutely necessary in all contingency cases, a human operator must be able to override the decision of the onboard system. The operator may decide, using all the information available, if the resources allow and if the situation is safe enough, just to interrupt the mission. Depending on the trajectory, this may be done by stopping the motion on the trajectory or by transferring the vehicle to a hold on V-bar and attempting to solve the problem there (for more details see chapter 9).